A Gravity Corrected Theory for Cylinder Withdrawal

DAVID A. WHITE and JOHN A. TALLMADGE

Yale University, New Haven, Connecticut

The speed range of the low-speed theory for cylinder withdrawal is extended by a correction for gravity and a modified use of the thin meniscus assumption. Experimental evidence indicates that this gravity corrected theory holds over a 3,000-fold range of speed, in terms of capillary number. This gravity corrected theory reduces, as special cases, to several other previously published theories as well as to the low-speed theory.

The problem of predicting entrainment in withdrawal of cylinders from liquid baths has been described previously (5, 9). In addition to theoretical importance, this problem is of practical interest in coating, pickling, washing, and lubrication operations. In 1965 (5) an empirical approach was developed for all radii for which data were available. It was found convenient to express both dimensionless film thickness and dimensionless entrainment flow as a function of dimensionless speed (N_{Ca}) and dimensionless radius (N_{Go}).

In 1966 (9) a low-speed theory was derived and verified for all radii and all liquids tested (except water) and for a range of capillary numbers. That theory was based on several approximations, which may be described in connection with the three regions shown in Figure 1. In addition to several conditions which can be obtained experimentally, the following assumptions were implied by the low speed theory development:

General assumption: (1) matching estimated curvatures from regions 2 and 3.

Region 3 assumption: (2) negligible viscous force.

Region 2 assumptions: (3) one-dimensional flow; (4) negligible effect of flow on the interfacial pressure change; (5) negligible radial curvature; (6) negligible film radius gradient; (7) thin meniscus; (8) negligible gravitational term.

However, significant deviations from the low-speed theory have been found at higher speeds, where $N_{Ca} > 0.03$. It is clear that extension of the theory is desirable.

The purpose of this paper is to develop and verify a new theory for predicting film thickness, one which is applicable over a wider range of capillary numbers and can be expressed as an analytical solution. The new theory, called a *gravity corrected theory*, is obtained by relaxing assumption 8 and modifying the use of assumption 7. It is much more general than the low-speed theory because it reduces to several previously described theories in addition to the low-speed theory.

LOW-SPEED THEORY FOR CYLINDERS

Because the new, gravity corrected theory is most easily understood when presented as an extension of the low-speed theory (9), the latter is briefly summarized below:

The low-speed theory is based on the Navier-Stokes equation for steady state, vertical withdrawal of cylinders from baths of wetting liquids. The flow is assumed to be laminar and ripple free. Under assumption 3, the equation for the x component reduces to the following expression for three forces:

$$\frac{d}{dx}(\sigma)\,(C_V^P - C_R^P) - \rho g + \frac{\mu}{r}\frac{d}{dr}\left(r\frac{du}{dr}\right) = 0 \qquad (1)$$

I. Surface tension (pressure) — II. Gravity force — III. Viscous force

Here C_V^P and C_R^P are principal curvatures in the vertical plane and radial direction, respectively (8).

Consider the three film regions of Figure 1. Region 1 is a constant thickness region; it occurs a few centimeters or so above the free surface (3). The first term vanishes and Equation (1) reduces to the familiar Nusselt type force balance for region 1:

$$\rho g - \frac{\mu}{r}\frac{d}{dr}\left(r\frac{du}{dr}\right) = 0 \qquad (2a)$$

By applying assumptions 4, 5, 6, and 8 in the second region, Equation (1) reduces to the following expression for the dynamic meniscus, region 2:

$$\sigma\frac{d}{dx}\left(\frac{d^2s}{dx^2}\right) + \frac{\mu}{r}\frac{d}{dr}\left(r\frac{du}{dr}\right) = 0 \qquad (2b)$$

When assumption 2 is applied close to the free surface, Equation (1) reduces to the expression for the static meniscus, region 3:

$$\sigma\frac{d}{dx}(C_V^P - C_R^P) - \rho g = 0 \qquad (3)$$

The method for predicting the film thickness (h_o) from these three equations involves the use of the usual wall and interface boundary conditions, $u = u_w$ at $r = R$ and

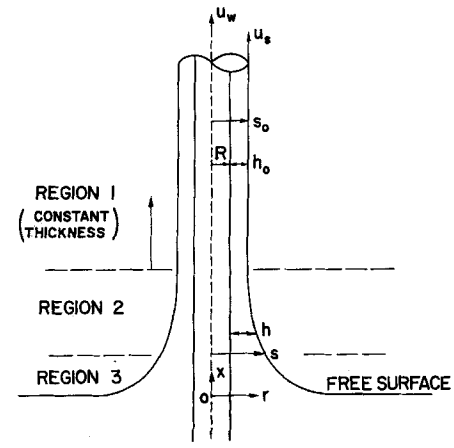

Fig. 1. Three regions of withdrawal.

David A. White is at University College, London, England. John A. Tallmadge is at Drexel Institute of Technology, Philadelphia, Pennsylvania.

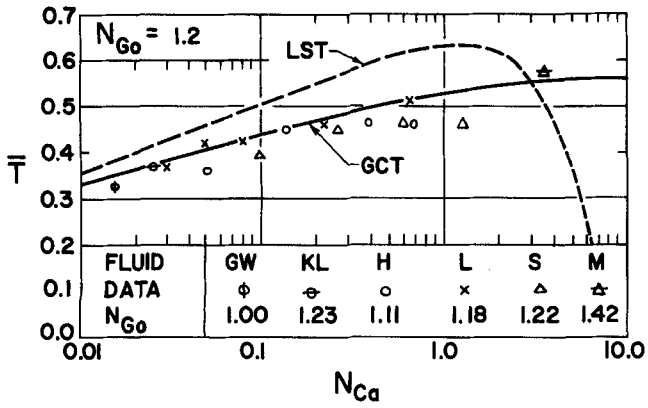

Fig. 2. Experimental results for rods (R = 0.318 and 0.346 cm.). ——— Gravity corrected theory (GCT). - - - - - Low-speed theory (LST).

$du/dr = 0$ at $r = s_o$. The third boundary condition is given by assumption 1, namely, $(d^2s/dx^2)_D = (d^2s/dx^2)_S$ at $x = x_{23}$ as used previously (3, 4, 7).

The curvature at the top of region 3 is calculated by solving Equation (3) for static conditions (8) and applying the theoretical solution to withdrawal (9). In the range of practical interest the curvature is given (9) by

$$\lim_{s \to s_o} \left(\frac{d^2s}{dx^2} \right)_s = \frac{2}{a} \left[\frac{2.4\, N_{Go}^{0.85}\, S_o^{0.85}}{1 + 2.4\, N_{Go}^{0.85}\, S_o^{0.85}} + \frac{1}{2\, N_{Go}\, S_o} \right] \quad (4)$$

The curvature at the bottom of region 2 is estimated from numerical integration of a third-order differential equation, simplified by using the thin meniscus assumption 7. The three boundary conditions are given in Appendix A and the derivation is presented in Appendix B. For a cylinder this curvature is (9)

$$\lim_{s \to \infty} \left(\frac{d^2s}{dx^2} \right)_D = \frac{0.944 \sqrt{2}\, N_{Ca}^{2/3}}{R(S_o - 1)} \quad (5)$$

The equation predicting film thickness by the low-speed theory (9) is obtained by using assumption 1, that is, by matching the right-hand sides of Equations (4) and (5) and rearranging.

This derivation is a four-way extension of the Landau-Levich flat plate method (4). The extensions were based on inclusion of the radial curvature in region 3 (8), modification of the two flat plate curvatures to those for cylinders (9), and correction for gravity in region 1 (1).

Table 1. Experimental Conditions (New Runs)

Fluid symbol	H	M*	S
Fluid	Glycerine	Molasses	Motor oil
N_{Go}	1.11	0.355	0.0047
Fluid properties:			
Viscosity, poise	5.16	32.8	4.86
Density, g./cc.	1.254	1.41	0.901
Surface tension, dynes/cm.	60.6†	34.6‡	29.8†
Cap. length a, cm.	0.314	0.224†	0.260
Wire properties:			
Wire size	No. 3	No. 2	No. 6
Material	Glass	Brass	Constantin
Radius	0.346	0.0795	0.00122
No. of wires	1	1	4
Immersion depths, cm.	5, 10, 15	5, 10, 15	12.9

* One run was made with brass rod No. 1. (0.318-cm. radius, N_{Go} = 1.42).
† Calculated.
‡ Knife edge tensiometer (6).

A GRAVITY CORRECTED THEORY: DEVELOPMENT OF THE EQUATION

This corrected theory is based on a modification of Equation (2b) by removing assumption 8 and using assumption 7 differently. The result is a revised third-order differential flow equation, and from it a new expression for dynamic curvature in place of Equation (5). The expression for static curvature, Equation (4), remains unchanged.

The first step in this derivation is the reintroduction of gravity into Equation (2b). Thus the region 2 equation becomes a *gravity corrected* expression:

$$\sigma \frac{d}{dx} \left(\frac{d^2s}{dx^2} \right) - \rho g + \frac{\mu}{r} \frac{d}{dr} \left(r \frac{du}{dr} \right) = 0 \quad (6)$$

The second step is the determination of the flow equation in the usual way (3, 7). This involves integrating Equations (2a) and (6) twice to get velocity profiles, a third time to get flow rates, and matching flow for regions 1 and 2 by continuity. After rearranging, one obtains the new differential equation for flow without any additional assumptions except the usual boundary conditions noted above.

$$F\left(\frac{s}{R}\right)\left(\frac{\sigma}{\mu u_w}\right)\left(s_o^2 \frac{d^3s}{dx^3}\right) = \left[\left(\frac{s}{s_o}\right)^2 - 1\right]\left(\frac{s_o}{R}\right)^4 - \left(\frac{s_o^2 \rho g}{\mu u_w}\right)\left[F\left(\frac{s}{R}\right) - F\left(\frac{s_o}{R}\right)\right] \quad (7)$$

where the F function (5) is defined by

$$F\left(\frac{s}{R}\right) \equiv \frac{1}{2}\left(\frac{s}{R}\right)^4 \left[\ln\left(\frac{s}{R}\right) - \frac{3}{4}\right] + \frac{1}{2}\left(\frac{s}{R}\right)^2 - \frac{1}{8} \quad (8)$$

Flow Equation (7) was rewritten by substituting definitions to obtain

$$\frac{F\left(\frac{s}{R}\right)}{N_{Ca}}\left(s_o^2 \frac{d^3s}{dx^3}\right) = \left[\left(\frac{s}{s_o}\right)^2 - 1\right] S_o^4 - D_o^2 \left[F\left(\frac{s}{R}\right) - F(S_o)\right] \quad (9)$$

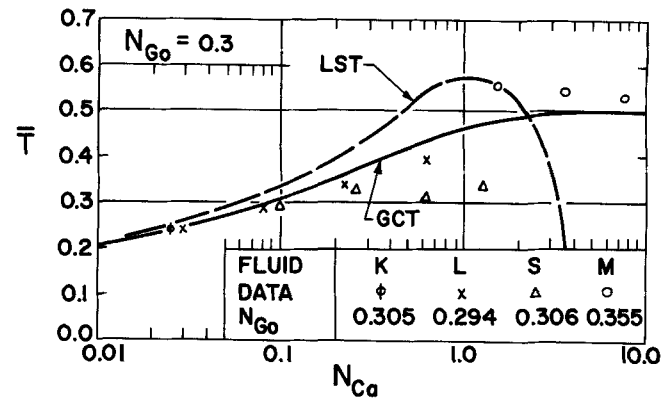

Fig. 3. Experimental results for large wires (R = 0.0795 cm.). ——— Gravity corrected theory (GCT). - - - - - Low-speed theory (LST).

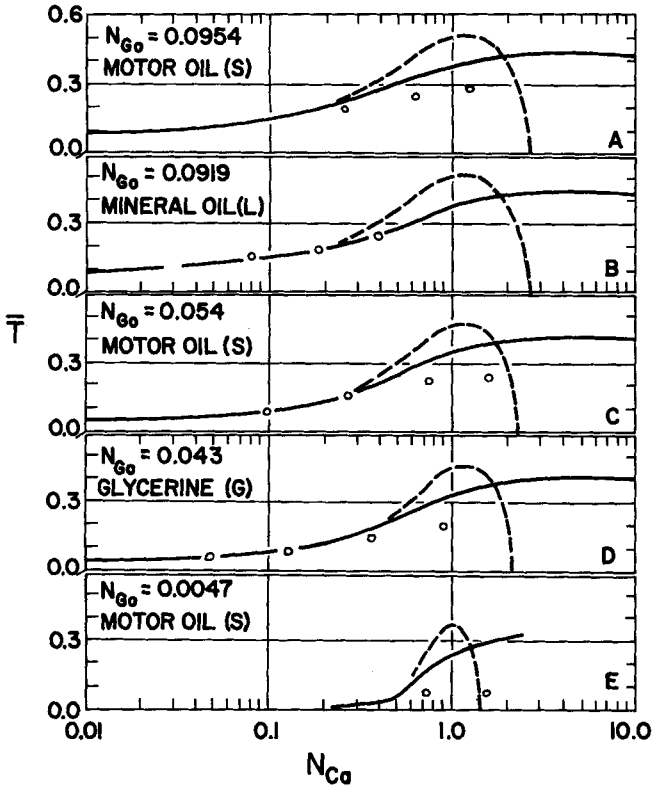

Fig. 4. Experimental results for small wires (R = 0.0248 to 0.0012 cm.). ——— Gravity corrected theory (GCT). - - - - - Low-speed theory (LST).

This equation was then solved for curvature by using thin meniscus assumption 7. Because this assumption of $(h/r << 1)$ is an important restriction, we discuss it in detail in Appendix A. As shown in Appendix A, the region 2 curvature in the vertical plane is

$$\lim_{s \to \infty} \left(\frac{d^2s}{dx^2}\right)_D = \frac{0.944\sqrt{2}\,N_{Ca}^{2/3}}{R(S_o - 1)}\,[1 - D_o^2 Z_o]^{2/3} \tag{10}$$

where

$$Z_o = \ln S_o - \frac{1}{2}\left(1 - \frac{1}{S_o^2}\right) \tag{11}$$

We then match Equations (10) and (4) by assumption 1 and rearrange to get

$$\frac{(S_o - 1)\,N_{Go}\sqrt{2}}{\sqrt{N_{Ca}}}\left[\frac{2.4\,N_{Go}^{0.85}\,S_o^{0.85}}{1 + 2.4\,N_{Go}^{0.85}\,S_o^{0.85}} + \frac{1}{2\,N_{Go}\,S_o}\right] = 0.944\,N_{Ca}^{1/6}$$

$$\left[1 - \frac{2\,S_o^2\,N_{Go}^2}{N_{Ca}}\left\{\ln S_o + \frac{1}{2\,S_o^2} - \frac{1}{2}\right\}\right]^{2/3} \tag{12a}$$

Equation (12a) is the gravity corrected theory for predicting film thickness on cylinders. It is an approximate solution, of general validity, to Equation (7).

Table 2. A Comparison of the Range of Validity for Two Theories

Wire size	Approximate upper limit			
	Low-speed theory		Gravity corrected theory	
N_{Go}	N_{Ca} limit	Ref.	N_{Ca} limit	Ref.
∞	0.03	7	2.0	7
1.2	0.03+	9	0.6+	This work
0.3	0.09	9	0.6	This work
0.1	0.2	9	0.3	This work
0.05	0.3	9	0.3	This work
Minimum overall upper limit	0.03		0.3	
Applicable range of N_{Ca}*	300-fold		3,000-fold	

* Based on a lower limit of N_{Ca} = 0.0001 for all N_{Go}.

COMPARISON WITH PREVIOUS THEORIES

The approximations used in deriving (12a) seem to be severe. We validate this equation by comparison with previously derived theoretical expressions and with experimental results. First we invoke a few identities:

$$T_o \equiv (S_o - 1)\,N_{Go}\sqrt{2}/\sqrt{N_{Ca}} \tag{13a}$$

$$C_S \equiv \frac{2.4\,N_{Go}^{0.85}\,S_o^{0.85}}{1 + 2.4\,N_{Go}^{0.85}\,S_o^{0.85}} + \frac{1}{2\,N_{Go}\,S_o} \tag{13b}$$

$$D_o = 2\,S_o^2\,N_{Go}^2/N_{Ca} \tag{13c}$$

These identities enable us to put Equation (12a) in the following short form:

$$T_o C_S = 0.944\,N_{Ca}^{1/6}\,[1 - D_o^2\,Z_o]^{2/3} \tag{12b}$$

At small N_{Go}, $(1/Cs) \to 2\,N_{Go}\,S_o$ and $D_o^2 Z_o \to 0$. Thus Equation (12b) becomes the previously verified small wire theory (9):

$$H_o = \frac{1.33\,N_{Ca}^{2/3}}{1 - 1.33\,N_{Ca}^{2/3}} \tag{14}$$

At large N_{Go}, $C_s \to 1$ and $D_o^2 Z_o \to T_o$. Thus Equation (12b) takes the form of the previously verified gravity corrected theory for flat plates (7).

$$T_o = 0.944\,N_{Ca}^{1/6}\,(1 - T_o^2)^{2/3} \tag{15}$$

Moreover Equation (15) reduces to the flat plate theories (7) for low-speeds ($T_o = 0.944\,N_{Ca}^{1/6}$ at low N_{Ca}) and for medium speeds ($T_o = 1$ at high N_{Ca}).

At small N_{Ca}, $D_o^2\,Z_o \to 0$, and Equation (12b) reduces to the previously verified low-speed theory for cylinders (9).

$$T_o\,C_s = 0.944\,N_{Ca}^{1/6} \tag{16}$$

Comparison of Equation (16) with (12b) shows that the $[1 - D_o^2 Z_o]^{2/3}$ group is the gravity correction.

At large N_{Ca}, $(T_o\,C_s/0.944\,N_{Ca}^{1/6}) \to 0$, so that Equation (12$b$) becomes

$$D_o^2\,Z_o = 1 \tag{17}$$

Equation (17) is equivalent to the drainage relationship reported previously (2) [as Equation (26)], with the use of the $u_w = (x/t)$ drainage-withdrawal transforma-

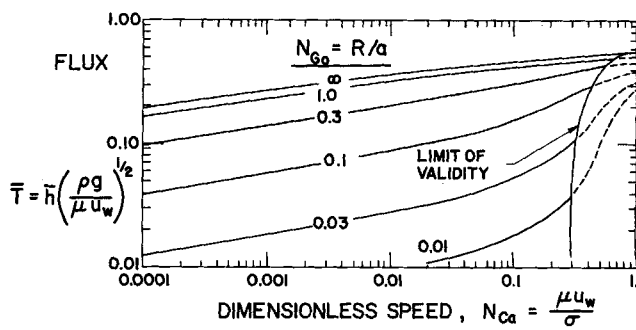

Fig. 5. Prediction of entrainment liquid by the gravity corrected theory, Equation (19).

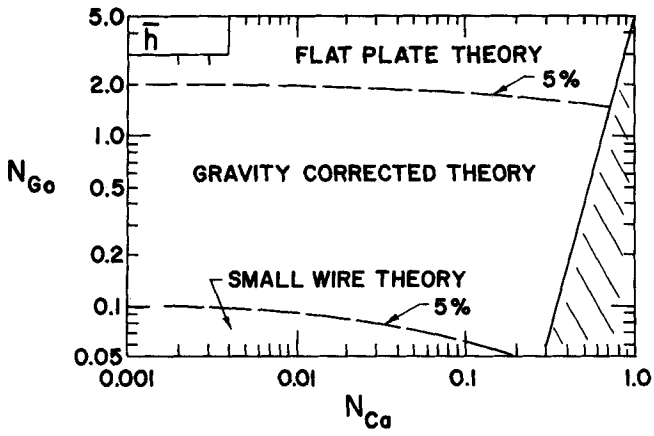

Fig. 6. Applicable flux equations for design. Flat plate: Equations (15) and (20), 5% criterion. Gravity corrected: Equation (19). Small wire: Equation (14), 5% criterion.

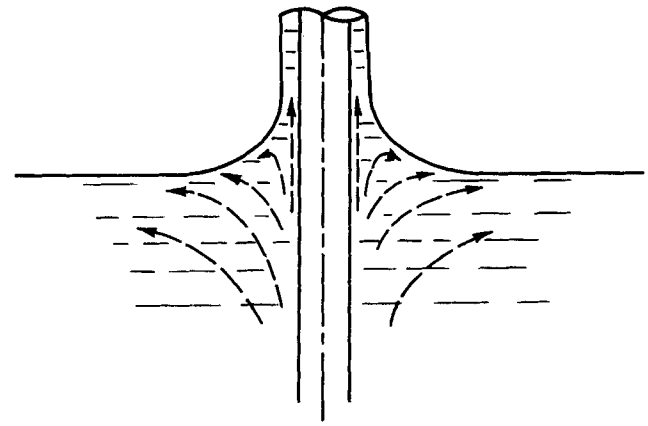

Fig. 7. Observed flow field.

tion. Equation (17) is a medium-speed theory for cylinders; it has not been compared with experimental data.

We conclude that the gravity corrected theory for cylinders reduces to many special cases, the low-speed theory for cylinders and three others.

EXPERIMENTAL VERIFICATION

Most of the relevant data were obtained by withdrawing short cylinders and determining mass by a gravimetric method (9). The form of dimensionless flow most sensitive for comparison with data is $\overline{T}$:

$$\overline{T} \equiv \left(\frac{\rho g}{\mu u_w}\right)^{1/2} \left[\frac{2}{u_w(s_o + R)}\right] \int_R^{s_o} ur\,dr \quad (18)$$

Equation (18) has been evaluated (5, 9). Thus with predicted thicknesses available from Equation (12*a*), one can predict flow rates:

$$\overline{T} = \overline{M}\,(N_{Ca}, N_{Go}) \quad (19)$$

The previously reported data theory comparison of the gravity corrected theory for flat plates (7) verified that theory, and therefore Equation (19), for large N_{Go} (2 to ∞), where $0.0001 \leq N_{Ca} \leq 2$. Likewise, the satisfactory comparison of data with the low-speed theory for cylinders (9) is taken as verification of Equation (19) for small and medium N_{Go} (0.05 to 1.2), where $0.0003 \leq N_{Ca} \leq 0.03$.

Because the gravity corrected theory has already been substantiated for wide ranges as noted above, we restrict our study of data to the untested region, namely, that at higher speeds ($N_{Ca} > 0.01$) and with radii smaller than flat plates ($N_{Go} < 2$). In addition to twenty-two runs in this region reported in the low-speed paper (9), ten new runs are used. These ten runs (Table 4*) were obtained with the same removal apparatus and method reported previously (9) and with the fluids and wires described in Table 1. Fluid symbols *K*, *L*, and *G* represent kerosene, mineral oil, and glycerine, respectively; *GW* and *KL* represent mixtures of glycerine-water and kerosene-mineral oil (9).

Figure 2 shows that for 3-mm. radius rods, the gravity corrected theory extends the speed range and improves the theoretical predictions. The upper limit of applicability is increased from a N_{Ca} of 0.03, for the low-speed theory, to 0.6 or more, with the 14% precision criterion (9). The median $\overline{T}$ deviation of theory from experiment is reduced from 26 to 6% for the eleven points in Figure 3 with N_{Ca} between 0.03 and 0.6 and from 14 to 5% for the twelve data points (Table 5*) in the low-speed region of $N_{Ca} < 0.03$.

Figure 3 confirms for 0.8-mm. radius wires, the trends noted in Figure 2. Specifically, the gravity correction raises the validity limit from a N_{Ca} of 0.09 to about 0.6. The median deviation of theory from experiment was reduced from 25 to 8% for the four Figure 3 runs with $0.09 < N_{Ca} < 0.6$ and from 4 to 1% for the five runs (Table 6*) with $N_{Ca} < 0.09$.

The molasses data in Figure 3 were taken at speeds which are considered above the valid limits. However, results seem to support the general shape of gravity corrected theory curve, especially above N_{Ca} of 4 where the low-speed $\overline{T}$ vanishes.

Based on Figure 4, it is clear that the gravity correction improves the theoretical prediction for small wires. However, the upper limit is not appreciably changed. Both data for $N_{Go} = 0.0047$ were taken at high speeds for experimental purposes (to entrain measureable masses). The sizable deviations shown may be related to assumption 5.

The upper limits determined for each wire size are reviewed in Table 2. On an overall basis for all Goucher numbers, the gravity corrected theory has extended the upper limit tenfold, from 0.03 to 0.3 in capillary number.

RANGE AND USE OF THEORY

Combining the speed limits shown in Table 2 with other validity conditions noted recently (9), we conclude that this gravity corrected theory predicts fluxes for all oily fluids tested, all radii tested, and all speeds up to $N_{Ca} = 0.3$. For larger cylinders, it applies for speeds up to $N_{Ca} = 2$. It apparently does not apply for water (9) and may or may not hold for aqueous solutions.

Values of $\overline{T}$ predicted by this gravity corrected theory for cylinders are shown in Figure 5. For design purposes, we suggest that fluxes should be determined by using one of three theories for the ranges shown in Figure 6. Equation (14) may be used to predict flux in the small wire region, since $\overline{h} = h_o$ in this region. To predict flux for flat plates as in Figure 6, it is necessary to use the flux-film thickness relationship for flat plates (7), Equation (20), in conjunction with Equation (15):

$$\overline{T} = T_o\,(1 - 0.5\,T_o^2) \quad (20)$$

The prediction of film thickness is further restricted to regions where droplets do not form. (These regions do

* Data Table 4 as well as Tables 5 to 11 and Appendix *C* have been deposited as document 9437 with the American Documentation Institute, Photoduplication Service, Library of Congress, Washington 25, D. C., and may be obtained for $1.25 for photoprints or 35-mm. microfilm.

* All data reported here and previously (9) are compared tabularly with both theories in Tables 5 to 9; see footnote in column 1.

TABLE 3. PREDICTED FILM THICKNESSES (GRAVITY CORRECTED THEORY)

Tabular values of the theoretical Equation (21), $T_o = M_o\ (N_{Ca}, N_{Go})$ (in units of $T_o \times 10^3$)

N_{Ca} \ N_{Go}	0.01 (c)	0.02 (c)	0.03 (c)	0.06 (c)	0.1 (c)	0.2 (c)	0.3	0.6	1.0	2.0	3.0	∞ (a)
0.0001	(b)	(b)	(b)	(b)	39	71	95	139	166	187	193	198
0.0003	(b)	(b)	(b)	(b)	47	85	114	167	197	222	230	235
0.001	(b)	(b)	(b)	35	57	104	139	202	238	268	276	282
0.003	(b)	(b)	(b)	43	70	126	167	240	282	315	325	332
0.01	(b)	(b)	(b)	55	88	156	206	291	337	374	384	392
0.03	(b)	(b)	(b)	70	112	194	252	345	394	432	444	452
0.1	(b)	(b)	53	102	158	258	321	415	463	501	512	521
0.2	(b)	52	76	141	207	312	373	460	505	540	551	561
0.3	(b)	73	105	181	251	352	407	487	529	564	574	585
0.4	*	*	*	*	*	382	433	507	547	580	590	601
0.6	*	*	*	*	*	*	*	534	570	602	612	624
0.8	*	*	*	*	*	*	*	*	*	*	628	640
1.0	*	*	*	*	*	*	*	*	*	*	*	652

a, calculated from flat plate Equation (15); *b*, accurately described by small wire Equation (14), based on a 1% criterion (see Figure 6 for the 5% criterion region); *c*, drops may form on small wires.
* Beyond the applicable limit on speed, based on a 14% criterion; see Figure 5.

not influence predicted or measured fluxes.) These regions are not well defined (9) but apparently include all the small wire region shown in Figure 6.

Tabular values of predicted film thickness are given in Table 3 as the M_o function. The M_o function is given by Equation (21), which is based on the gravity corrected theory prediction [Equation (12*a*)] and the definition of T_o [Equation (13*a*)].

$$T_o = M_o\ (N_{Ca}, N_{Go}) \qquad (21)$$

Tabular values of predicted $\overline{T}$ flux [the $\overline{M}$ function of Equation (19)] and the predicted ratio of $\overline{h}/h_o\ (= \overline{M}/M_o)$ are given elsewhere (Tables 10 and 11*).

DISCUSSION OF ASSUMPTIONS

The assumptions made in deriving the gravity corrected theory are examined below in numerical order.

1. There is no approximation, per se, in *matching curvatures* since the curvature is a continuous function. The approximation arises in the estimates. The relevance of the estimates, such as Equations (4) and (5), has been justified by the mass and thickness data noted here and elsewhere. However, these estimates may be an important restriction for some conditions, such as non-Newtonian fluids (3) and high speeds.

2. *Neglect of the viscous term* in region 3 implies that the lower part of the actual meniscus is similar in shape to that at zero flow. This has been substantiated by visual observations at slow speeds (3) but does not appear to hold at higher speeds. This approximation also implies a negligible effect of the flow field below the free surface. Since the flow in the meniscus is similar to that of Figure 7, the effect of the flow field will probably be more important at higher speeds.

3. The *one-dimensional flow* assumption for region 2 is least valid at the estimated match point. It is, however, a good approximation near region 1, where the largest change in curvature occurs in many systems. Nonconsideration of the constraint of the radial-component equation of motion is probably valid over a wide speed range, but neglect of inertial force is probably not applicable at higher speeds.

4. The *pressure change* across the interface will be affected, where mixtures are present, by fresh surface effects due to the flow field (Figure 7). This dynamic surface-tension effect does not, however, seem to account for the water paradox (8). This effect and flow deviations from the LaPlace's equation would probably be more severe at higher speeds.

5. The effect of *radial curvature* is discussed elsewhere (Appendix C*).

6. The *gradient of film radius* in region 2 (ds/dx) is negligible compared to unity in the vicinity of region 1. This gradient becomes larger closer to the free surface, but it is still small if the assumption 1 match point is not too large. One estimate of the match point is available (Appendix C*).

7. The assumption of a *thin meniscus* in region 2 ($h/R << 1$) implies a *thin film* assumption in region 1, $h_o/R << 1$ (because $h_o \leq h$), but the converse is not generally valid. The thin meniscus assumption also implies a *linear film radius* assumption in region 2, $e = (S_o - 1) << 1$ [because $e \equiv (H + H_o)/(1 + H_o)$], but the converse is not generally valid. The way these three assumptions are involved is shown in Appendix A (gravity corrected theory) and Appendix B (low-speed theory).

SUMMARY

1. A gravity corrected theory for cylinder withdrawal is developed, experimentally verified, and presented in Figure 5. It has been found valid for all radii (N_{Go}) tested, all oily liquids tested, and for $N_{Ca} \leq 0.3$.

2. The gravity corrected theory is a general one in the sense that it reduces to six other published withdrawal theories as special cases, four directly and two indirectly.

3. A design procedure for predicting flow (Figure 6) and film thickness (Table 3) is suggested, with the use of two of the special cases of the theory. Use of the theory to predict film thickness is more limited than that for flow because of droplet formation.

ACKNOWLEDGMENT

This work was supported by a fellowship from Chevron Research Company and in part by National Science Foundation Grant GK-1201.

NOTATION

a = capillary length, $(2\,\sigma/\rho\,g)^{1/2}$
B_1 = dimensionless coordinate, $-\,xN_{Ca}^{1/3}/s_o$
C_R^P = principal curvature, radial direction, cm^{-1}
C_S = top curvature of a static meniscus on a radius s_o, dimensionless

* See footnote on page 748.
* See footnote in column 1.

C_V^P = principal curvature, vertical plane, cm.$^{-1}$
D_o = dimensionless film radius, $s_o(\rho g/\mu u_w)^{1/2}$
e = $(s/s_o) - 1$
F = function given by Equation (8)
g = gravitational acceleration, cm./sec.^{2}
h, h_o = film thickness, $s - R$, $s_o - R$, cm.
$\bar{h}$ = flow thickness, $\bar{s} - R$, cm.
H, H_o = dimensionless thickness, h/R *and* h_o/R
$M_o, \bar{M}$ = gravity corrected theory, Equations (19) and (21)
N_{Ca} = capillary number (dimensionless speed), $\mu u_w/\sigma$
N_{Go} = Goucher number (dimensionless radius), R/a
r = radial coordinate
R = wire radius, cm.
s = film radius at any point, cm.
$\bar{s}$ = flow radius, $R + \bar{T}(\mu u_w/\rho g)^{1/2}$, cm.
s_o = film radius in region 1, cm.
S, S_o = dimensionless film radius, s/R and s_o/R
t = time, sec.
T_o = dimensionless thickness, $(s_o - R)(\rho g/\mu u_w)^{1/2}$
$\bar{T}$ = dimensionless flow, given by Equation (18)
u_w = wire withdrawal speed, cm./sec.
x = vertical coordinate
Z_o = function of S_o, defined by Equation (11)

Greek Letters

μ = viscosity, poise
ρ = density, g./cc.
σ = surface tension at the liquid-gas interface, dyne/cm.

LITERATURE CITED

1. Derayagin, B. V., and A. S. Titiyevskava, *Dokl. Akad. Nauk SSSR*, **50**, 307 (1945).
2. Gutfinger, Chaim, and J. A. Tallmadge, *AIChE J.*, **10**, 774 (1964).
3. *Ibid.*, **11**, 403 (1965).
4. Landau, L. D., and V. G. Levich, *Acta Physiochem. URSS*, **17**, No. 1-2, 41 (1942).
5. Tallmadge, J. A., R. A. Labine, and B. H. Wood, *Ind. Eng. Chem. Fundamentals Quart.*, **4**, 400 (1965).
6. White, D. A., Ph.D. dissertation, Yale Univ., New Haven, Conn. (Apr., 1965).
7. ———, and J. A. Tallmadge, *Chem. Eng. Sci.*, **20**, 33 (1965).
8. ———, *J. Fluid Mech.*, **23**, 325 (1965).
9. ———, *AIChE J.*, **12**, 333 (1966).

APPENDIX A CURVATURE FROM THE DIFFERENTIAL FLOW EQUATION (9)

We replace the s and x coordinates in Equation (9) with $L = s/s_o$ and $B_1 = -xN_{Ca}^{1/3}/s_o$. (The B_1 variable also changes the x axis direction to downward.) Thus

$$F(LS_o)\frac{d^3L}{dB_1^3} = (L^2 - 1)S_o^4 - D_o^2[F(LS_o) - F(S_o)] \quad (A1)$$

where*

$$L = 1, \frac{dL}{dB_1} = 0, \text{ and } \frac{d^2L}{dB_1^2} = 0 \text{ at } B_1 = 0 \quad (A2)$$

Substituting $(1 + H)$ into the left side (LS_o) and $(1 + e)$ into other values of L, we obtain

$$F(1 + H)\frac{d^3e}{dB_1^3} = (2e + e^2)S_o^4 - D_o^2[F\{(1 + e)S_o\} - F(S_o)] \quad (A3)$$

By assuming a *linear film radius,* it follows from Equation (8) that $F[(1 + e)S_o] = F(S_o) + 2e\,S_o^4Z_o + O(e^2)$. Thus, neglecting higher order e terms, one obtains

$$F(1 + H)\frac{d^3e}{dB_1^3} = 2e\,S_o^4[1 - D_o^2Z_o] \quad (A4)$$

We can write this in form of the low-speed theory, Equation (B1), by a change of coordinate

$$B_2^3 = (1 - D_o^2Z_o)B_1^3 \quad (A5)$$

With this change, Equation (A4) becomes

$$F(1 + H)\frac{d^3e}{dB_2^3} = 2e\,S_o^4 \quad (A6)$$

which is the same form as Equation (B1). Assuming that Equations (A6) and (B1) have approximately the same solution (even when e is not small), we take the solution for curvature on a B_2 coordinate scale, from Equation (B5). Thus

$$\left(\frac{d^2s}{dx_2^2}\right)_D = \frac{0.944\sqrt{2}\,N_{Ca}^{2/3}}{R(S_o - 1)} \quad (A7)$$

Where the relationship between coordinates is $(x_2/x) = (B_2/B_1)$. From Equation (A5)

$$\frac{B_2}{B_1} = [1 - D_o^2Z_o]^{1/3} \quad (A8)$$

so that

$$\left(\frac{d^2s}{dx^2}\right)_D = \left(\frac{d^2s}{dx_2^2}\right)_D [1 - D_o^2Z_o]^{2/3} \quad (A9)$$

Substitution of Equation (A7) into (A9) leads to the gravity corrected theory expression, Equation (10).

Parenthetically, we note that the gravity corrected theory may also be obtained by relaxing one aspect of the *thin meniscus* assumption. Consider the gravity correction term in Equation (A4). If we assume a *thin film,* then

$$D_o^2Z_o = D_o^2[H_o^2 + O(H_o^3) + \ldots.] \quad (A10)$$

If we further assume that $H_o \to 0$, then $D_o^2Z_o \to 0$ and Equation (A4) reduces to the low-speed theory form of Equation (A6).

APPENDIX B THE THIN MENISCUS ASSUMPTION (THE LOW-SPEED THEORY)

When gravity is negligible so that $D_o^2Z_o \to 0$, Equation (A4) reduces to the low-speed theory form

$$F(1 + H)\frac{d^3e}{dB_1^3} = 2e\,S_o^4 \quad (B1)$$

Now we assume a *thin meniscus,* from which it follows from Equation (8) that $F(1 + H) = \frac{2}{3}H^3 + O(H^4)$. Neglecting higher order terms, we see that Equation (B1) becomes

$$\frac{d^3e}{dB_1^3} = \frac{3e\,S_o^4}{H^3} \quad (B2)$$

We change Equation (B2) to plate geometry by substituting $B_3^3 = 3(S_oB_1/H_o)^3$ and $Lp = H/H_o = (S_oe/H_o) + 1$. Thus

$$\frac{d^3Lp}{dB_3^3} = \frac{(Lp - 1)(1 + H_o)}{Lp^3} \quad (B3)$$

By assuming a *thin film,* Equation (B3) reduces to

$$\frac{d^3Lp}{dB_3^3} = \frac{Lp - 1}{Lp^3} \quad (B4)$$

Equation (B4) is identical with that of flat plates (7), allowing for different coordinate directions. The limiting curvature at $x \to \infty$ predicted from Equation (B4) has been shown (7) to be $(d^2h/dx^2)D = 0.944\sqrt{2}\,N_{Ca}^{2/3}/h_o$. When applied to cylinders (9), this becomes Equation (B5):

$$\left(\frac{d^2s}{dx^2}\right)_D = \frac{0.944\sqrt{2}\,N_{Ca}^{2/3}}{R(S_o - 1)} \quad (B5)$$

Equation (B5) is given in the text as Equation (5).

Manuscript received June 3, 1966; revision received November 2, 1966; paper accepted November 2, 1966. Paper presented at AIChE Detroit meeting.

* A sign error on the gravity term is present in flat plate Equations (7), (10), and (12) of section 133 of "Physicochemical Hydrodynamics," by Levich, Prentice Hall, (1962). His dimensionless result is correct, however, because all signs in his L Equation (19) are proper and consistent with the implied upward direction of x. A similar sign error also appears in Equation (1) of another flat plate description (7), together with a sign error in the derivative term in Equation (2).